Tellus (1979), *31*, 254–268

Oscillating, stratified boundary layers driven by surface temperature variations

By SOON-UNG PARK and L. MAHRT, *Department of Atmospheric Sciences, Oregon State University, Corvallis, Oregon 97331, U.S.A.*

(Manuscript received September 6; in final form December 21, 1978)

ABSTRACT

A classification of types of stratified, rotating boundary layers, driven by periodic forcing is presented. The dynamics of such flow is shown to depend on the product of the Ekman number and a stratification parameter and on the ratio of the forcing frequency to the Coriolis frequency. Certain asymptotic solutions are presented for atmospheric values of the stratification parameter and mid-latitude-synoptic and diurnal values of the nondimensional forcing frequency. For the case of flow driven by diurnally varying, differential surface heating, the thermal forcing is absorbed primarily by the Stokes part of the flow which in turn generates an Ekman layer and associated vertical motion. This Ekman pumping induces adjustments in an overlying oscillating Lineykin layer.

1. Introduction

Most analytical investigations of boundary layer flow have considered either neutrally stratified, time-dependent flow or steady stratified flow. In geophysical flows, however, such effects occur simultaneously with important interactions. Kuo (1973) has considered such interactions for the case of synoptic scale oscillations. By considering certain simplifications to Kuo's system, the present analysis clarifies some of the physics of such interactions and extends the analysis to a wider range of oscillation frequencies to include, for example, diurnal oscillations.

In particular, this study focuses on boundary layers which are forced by time-dependent horizontal variations of surface temperature. In geophysical flows, such variations in surface temperature could be associated with horizontal variations in surface properties such as heat capacity, as might occur in land breezes and urban circulation systems or in any geographical location where surface conditions vary systematically. The study of Stommel and Veronis (1957) belongs to the steady-state limit of this flow problem. While we will examine a range of forcing frequencies and stratification values, we will emphasize mid-latitude, diurnally varying flows. Since we will investigate the physics of the linearized dynamics, it will be understood that the following solutions and discussions are not applicable to forcing frequencies near the Coriolis frequency (critical latitude). The ensuing analysis will also be limited to the case of finite stable stratification.

2. Governing equations

We assume the field variables to be independent of one horizontal direction and periodically dependent on the other horizontal direction, as for example, in Stommel and Veronis (1957), Leetmaa (1971), Hsueh and Kenny (1972), and Kuo (1973) and periodic with time as in Holton (1967) so that:

$$\left.\begin{aligned}[\tilde{u}, \tilde{v}] &= [u_*, v_*] \sin [x_*/L] \exp [-i\omega t_*] \\ [\tilde{p}, \tilde{\theta}, \tilde{w}] &= [p_*, \theta_*, w_*] \cos [x_*/L] \exp [-i\omega t_*]\end{aligned}\right\} \quad (1)$$

where u_*, v_*, p_*, θ_* and w_* are, respectively, the amplitudes of $\tilde{u}$, the dimensional eastward wind component, $\tilde{v}$, the northward wind component. $\tilde{p}$, the pressure, $\tilde{\theta}$, the potential temperature, and $\tilde{w}$, the vertical motion in Cartesian coordinates x_*, y_* and z_*. These amplitudes are functions of only

0040-2826/79/030254-15$02.50/0

height. Pressure and potential temperature are deviations from a static basic state which is only a function of height. t_* is time, L the horizontal length scale and ω the frequency of the flow. All variables in (1) are dimensional.

Assuming small amplitude (small Rossby number), Boussinesq, hydrostatic flow with constant eddy viscosity K and unity Prandtl number, the governing equations for the scaled, height-dependent amplitudes of the time-dependent horizontally periodic flow are:

$$-i\hat{\omega}u - v = p + \frac{E}{\delta^2}\frac{\partial^2 u}{\partial \eta^2} \tag{2a}$$

$$-i\hat{\omega}v + u = \frac{E}{\delta^2}\frac{\partial^2 v}{\partial \eta^2} \tag{2b}$$

$$\frac{\partial p}{\partial \eta} = \delta\theta \tag{2c}$$

$$-i\hat{\omega}\theta + B^2 w = \frac{E}{\delta^2}\frac{\partial^2 \theta}{\partial \eta^2} \tag{2d}$$

$$\delta u + \frac{\partial w}{\partial \eta} = 0 \tag{2e}$$

where $(u_*, v_*, w_*) = V\left(u, v, \frac{H}{L} w\right)$

$$x_* = Lx$$

$$z_* = \delta H \eta$$

$$p_* = fLV\rho_{00}\, p$$

$$\frac{\theta_*}{\theta_{00}} \equiv \frac{fLV}{gH}\theta$$

$$t_* = \omega^{-1} t$$

$$\hat{\omega} \equiv \frac{\omega}{f} \equiv \text{nondimensional frequency}$$

$$E \equiv \frac{K}{fH^2} \equiv \text{turbulent Ekman number}$$

$$B^2 \equiv \left(\frac{NH}{fL}\right)^2 \equiv \text{stratification parameter}$$

$$N \equiv \left(\frac{g}{\theta_{00}}\frac{d\theta_0}{dz_*}\right)^{1/2} \equiv \text{Brunt-Väisälä frequency}$$

All variables in (2) are nondimensional. The subscript o represents the height dependent, basic state thermodynamic variables while the subscript oo_{00} represents constant, basic state, scaling variables. V is the horizontal velocity scale, H is the scale height of the flow and δ is a stretching factor for the vertical coordinate, to be determined later. This system is similar to that examined by Kuo (1973) except here the Coriolis parameter f is assumed constant.

Combining eqs. (2a–e) we obtain a single eighth-order equation for perturbation pressure

$$\left(\frac{E}{\delta^2}\frac{\partial^2}{\partial \eta^2} + i\hat{\omega}\right) \times \left(\frac{\partial^6}{\partial \eta^6} + \frac{2\hat{\omega}\delta^2}{E} i \frac{\partial^4}{\partial \eta^4} + \frac{(1-\hat{\omega}^2)\delta^4}{E^2}\frac{\partial^2}{\partial \eta^2} - \frac{B^2\delta^6}{E^2}\right) \times p = 0 \tag{3}$$

The factor $((E/\delta^2)(\partial^2/\partial\eta^2) + i\hat{\omega})\, p$ represents the thermal Stokes boundary layer with oscillation frequency ω and dimensional boundary layer thickness $(2K/\omega)^{1/2}$. This layer is associated with temperature diffusion as discussed in Section 3.

We first consider the possible two-term balances (as in Blumsack and Barcilon, 1971) for the second parenthesis of eq. (3). The restriction that the remaining terms be small compared with those retained allows us to form restrictions among the governing parameters, B^2, E, and $\hat{\omega}$ defining the parameter regions depicted in Fig. 1. These restrictions can be compactly expressed in terms of $\hat{\omega}$ and $m = B^2E$. Subdivision of region II in Fig. 1 is facilitated by altering the principal balance in the thermodynamic equation (2d), which in turn

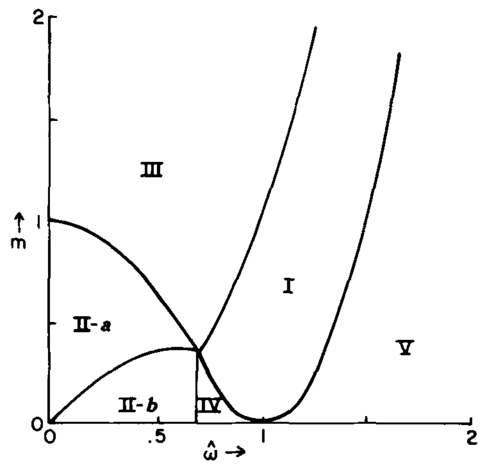

Fig. 1. Oscillating boundary layers in parameter space $(m, \hat{\omega})$. Subdivisions are facilitated by two-term balances in eq. (3).

depends upon the relative magnitude of the temporal and diffusion terms.

The six possible two-term balances are summarized in Table 1. Because the coefficients are complex and the phase of pressure is not known *a priori*, parameter restrictions and estimates of boundary layer depth can only be interpreted as order of magnitude quantities. In the atmosphere any one of the boundary layers listed in Table 1 may occur in nearly pure form or in combination with the other types of boundary layers.

More than one two-term balance may occupy the same region in $m - \hat{\omega}$ space but each balance corresponds to a different depth scale and different region above the ground. The approximate equations for each two-term balance are obtained in the following way. The depth scale is obtained by equating the coefficients of the two terms retained in the right parenthesis of eq. (3).

Height is rescaled with this depth. The approximate magnitudes of the various terms can then be found by allowing the dependent variables to be rescaled by starting with the hydrostatic equation, assuming θ is $O(1)$ and imposing approximations based on restrictions for $\hat{\omega}$ and m. Then certain terms in the equations with more than two terms can be neglected, resulting in the simplified equations in Table 1.

3. Thermally driven mid-latitude flows

3.1. *Governing equation*

We wish to obtain asymptotic solutions for flows driven by surface temperature variations of the dimensional form $\theta_*(0)\cos(x_*/L)\,e^{-i\omega t_*}$. The following boundary conditions are applied to the system (2):

$$\left.\begin{array}{ll} u, v, w = 0 \quad \theta = \theta(0) & \text{at } \eta = 0 \\ u, v, w, \theta \to 0 & \text{as } \eta \to \text{large} \end{array}\right\} \tag{4}$$

where $\theta(0) = (gH/fLV)(\theta_*(0)/\theta_{00})$ is the scaled amplitude of the potential temperature perturbation. If the motion is driven by surface temperature variations so that $\theta(0)$ is $O(1)$, then the characteristic, geostrophic, velocity amplitude V is order of $(gH/fL)(\theta_*(0)/\theta_{00})$. However, we must assume $\theta_*(0) \ll \Delta\theta_0$ to make the above perturbation assumption applicable, where $\Delta\theta_0$ is the basic state potential temperature thickness.

The following rescaling of variables can reduce the problem to a two-parameter system in m and $\hat{\omega}$ as indicated in Table 1:

$$\left.\begin{array}{l} \theta = \hat{\theta} \\ \delta = E^{1/2} \\ w = E\hat{w} \\ u = E^{1/2}\hat{u} \\ v = E^{1/2}\hat{v} \\ p = E^{1/2}\hat{p} \end{array}\right\} \tag{5}$$

Dropping the carot notation, eq. (3) assumes the form:

$$\left(\frac{\partial^2}{\partial\eta^2} + i\hat{\omega}\right)\left(\frac{\partial^6}{\partial\eta^6} + 2\hat{\omega}i\frac{\partial^4}{\partial\eta^4} + (1-\hat{\omega}^2)\frac{\partial^2}{\partial\eta^2} - m\right) \times p = 0 \tag{6}$$

Since the thermally driven flow vanishes at $\eta \to \infty$, we may assume the solution of eq. (6) to be of the form:

$$p = \sum_{i=1}^{4} C_i\, e^{-\alpha_i \eta} \tag{7}$$

where C_i is constant and the α_i's are the positive real roots of the following equation

$$(\alpha_i^2 + i\hat{\omega})(\alpha_i^6 + 2\hat{\omega}i\alpha_i^4 + (1-\hat{\omega}^2)\alpha_i^2 - m) = 0 \tag{8}$$

Further simplifications can be imposed by restricting attention to limited regions of $m - \hat{\omega}$ space. $\hat{\omega}$ is approximately 0.7 for mid-latitude diurnally-varying flows. m is normally expected to be small compared to one. However, before categorically imposing such a restriction, a relationship between K and N must be estimated since the turbulence is suppressed by the stratification.

3.2. *Dependence of exchange coefficients on stratification*

If the boundary layer above the surface layer is characterized by only one independent velocity and length scale then we can postulate:

$$\delta \propto \frac{u_*}{N} \tag{9}$$

$$u_* \equiv C_D V \tag{10}$$

where u_* is the surface friction velocity and C_D is a drag coefficient, u_*/N is the depth scale of a parcel

Table 1. *Oscillating stratified boundary layers*

Name	Dimensional thickness	Restriction regions	Relative order of magnitude u	v	w	θ	p	Scaled governing equation
Stokes	$\left(\frac{K}{\omega}\right)^{1/2}$	$\hat\omega \gg \frac{1}{\sqrt{2}}$, $m \ll \hat\omega^3$ I, IV, V	$\frac{\hat\omega(\hat\omega E)^{1/2}}{m}$	$\frac{(\hat\omega E)^{1/2}}{m}$	$\frac{\hat\omega E}{m}$	1	$\left(\frac{E}{\hat\omega}\right)^{1/2}$	$-iu - \frac{v}{\hat\omega^2} = \frac{d^2 u}{d\eta^2}$, $-i\theta + w = \frac{d^2\theta}{d\eta^2}$ $-iv + u = \frac{d^2 v}{d\eta^2}$, $u + \frac{dw}{d\eta} = 0$, $\frac{dp}{d\eta} = \theta$
Oscillating Ekman ($E^{1/2}$ layer)	$(K/\sqrt{f^2-\omega^2})^{1/2}$	$\hat\omega \ll \frac{1}{\sqrt{2}}$, $m \ll (1-\hat\omega^2)^{3/2}$ II-a, II-b	$E^{1/2}\frac{(1-\hat\omega^2)^{3/4}}{m}$	$E^{1/2}\frac{(1-\hat\omega^2)^{1/4}}{m}$	$E\frac{(1-\hat\omega^2)^{1/2}}{m}$	1	$\left(\frac{E}{\sqrt{1-\hat\omega^2}}\right)^{1/2}$	$-i\frac{\hat\omega}{\sqrt{1-\hat\omega^2}}u - \frac{v}{1-\hat\omega^2} = \frac{d^2u}{d\eta^2}$, $w = \frac{d^2\theta}{d\eta^2}$ $u = \frac{d^2 v}{d\eta^2}$, $u + \frac{dw}{d\eta} = 0$, $\frac{dp}{d\eta} = \theta$
$E^{1/3}$ layer	$(KL/N)^{1/3}$	$m \gg \hat\omega^3$ $m \gg (1-\hat\omega^2)^{3/2}$ III	$\left(\frac{E}{m}\right)^{1/2}$	$\left(\frac{E^3}{m^5}\right)^{1/6}$	$\left(\frac{E^3}{m^2}\right)^{1/3}$	1	$\left(\frac{E^3}{m}\right)^{1/6}$	$-v = m^{2/3}\left(p + \frac{d^2u}{d\eta^2}\right)$, $w = \frac{d^2\theta}{d\eta^2}$, $u = \frac{d^2 v}{d\eta^2}$, $u + \frac{dw}{d\eta} = 0$, $\frac{dp}{d\eta} = \theta$
Stokes–Ekman ($E^{1/2}$ layer)	$\lvert K\omega/(f^2-\omega^2)\rvert^{1/2}$	$\hat\omega \gg \frac{1}{\sqrt{2}}$, $m \ll \frac{(1-\hat\omega^2)^2}{\hat\omega}$ IV	$\left[\frac{E\hat\omega(1-\hat\omega^2)}{m^2}\right]^{1/2}$	$\lvert E(1-\hat\omega^2)/m^2\hat\omega\rvert^{1/2}$	$\hat\omega E/m$	1	$\lvert E\hat\omega/(1-\hat\omega^2)\rvert^{1/2}$	$-i\hat\omega^2 u - v = (1-\hat\omega^2)\frac{d^2u}{d\eta^2}$, $-i\theta + w = 0$ $-iv + u = 0$, $u + \frac{dw}{d\eta} = 0$, $\frac{dp}{d\eta} = \theta$
Stokes–$E^{1/3}$ ($E^{1/4}$ layer)	$(K\omega L^2/N^2)^{1/4}$	$m \ll \hat\omega^3$, $m \gg \frac{(1-\hat\omega^2)^2}{\hat\omega}$ I	$\left[\frac{E^2\hat\omega^3}{m^3}\right]^{1/4}$	$\left[\frac{E^2}{m^3\hat\omega}\right]^{1/4}$	$\frac{\hat\omega E}{m}$	1	$\left[\frac{E^2\hat\omega}{m}\right]^{1/4}$	$p + \frac{d^2u}{d\eta^2} = 0$, $-i\theta + w = 0$, $u = iv$, $u + \frac{dw}{d\eta} = 0$, $\frac{dp}{d\eta} = \theta$
Oscillating Lineykin layer	$\frac{fL}{N}\sqrt{1-\left(\frac{\omega}{f}\right)^2}$	$m \ll (1-\hat\omega^2)^{3/2}$ $m \ll \frac{(1-\hat\omega^2)^2}{\hat\omega}$ $m < \hat\omega(1-\hat\omega^2)$ II-b, IV	$\left(\frac{\hat\omega^2 E}{m(1-\hat\omega^2)}\right)^{1/2}$	$\left(\frac{E}{m(1-\hat\omega^2)}\right)^{1/2}$	$\frac{\hat\omega E}{m}$	1	$\left[\frac{(1-\hat\omega^2)E}{m}\right]^{1/2}$	$-i\hat\omega^2 u - v = (1-\hat\omega^2)\,p$, $-i\theta + w = 0$ $-iv + u = 0$, $u + \frac{dw}{d\eta} = 0$, $\frac{dp}{d\eta} = \theta$
		$m \ll (1-\hat\omega^2)^{3/2}$ $m \ll (1-\hat\omega^2)^2/\hat\omega$ $m > \hat\omega(1-\hat\omega^2)$ II-a	$\left(\frac{mE}{(1-\hat\omega^2)^3}\right)^{1/2}$	$\left(\frac{E}{m(1-\hat\omega^2)}\right)^{1/2}$	$\frac{E}{1-\hat\omega^2}$	1	$\left[\frac{(1-\hat\omega^2)E}{m}\right]^{1/2}$	$-v = (1-\hat\omega^2)\,p$, $w = \frac{d^2\theta}{d\eta^2}$ $u = \frac{d^2 v}{d\eta^2}$, $u + \frac{dw}{d\eta} = 0$, $\frac{dp}{d\eta} = \theta$

with initial kinetic energy u_*^2. If we assume that the eddy diffusivity is proportional to the turbulent velocity and length scales (e.g., Zilitinkevich et al., 1967), eqs. (9) and (10) then imply that

$$K = Cu_*^2/N \tag{11}$$

$$m = \frac{N^2 K}{f^3 L^2} \equiv \frac{CNC_D^2 V^2}{f^3 L^2} \tag{12}$$

where C is a nondimensional constant. The parameter m varies only as the square root of the stratification $d\theta_0/dz_*$ along with a possible compensating inverse dependence of C_D on stratification. Considering different types of mid-latitude flows, m seems to be more sensitive to the horizontal length scale than to the stratification; that is small scale flows are more strongly influenced by a given stratification than large scale flows.

For example, consider the strongly stratified case where $N = 2 \times 10^{-2}\ \mathrm{s}^{-1}$. If we also choose $C_D = 10^{-2}$, $V = 3\ \mathrm{ms}^{-1}$, $f = 10^{-4}\ \mathrm{s}^{-1}$ and $C = 1$, then m is small compared to one if L is large compared to 4.5 km. If stratification is decreased by a factor of 4, then this critical length scale is 2.25 km.

3.3 *Approximation for small m*

We proceed to solve (8) with the restrictions of parameters; $\hat{\omega} < 1$, $m \ll (1 - \hat{\omega}^2)^{3/2}$ and $m\hat{\omega} \ll (1 - \hat{\omega}^2)^2$. Strictly speaking, these restrictions correspond, respectively, to small subregions of flow regimes II-a, II-b, and IV in Fig. 1. The roots to (8) are obtained by guessing one root to correspond to the depth of the oscillating Lineykin layer (Table 1) and using Newton's iterative method to obtain the three roots to lowest order. Using this procedure, we obtain

$$\left.\begin{aligned} \alpha_s &= \left(\frac{\hat{\omega}}{2}\right)^{1/2}(1 - i) \\ \alpha_L^2 &= \frac{m}{1 - \hat{\omega}^2} + O(m^2) \\ \alpha_{1,2}^2 &= \frac{-m}{2(1 - \hat{\omega}^2)} - (\hat{\omega} \pm 1)\, i + O(m^2) \end{aligned}\right\} \tag{13}$$

α_s, α_L and $\alpha_{1,2}$ are identified respectively, as the inverse thickness of the thermal Stokes, oscillating Lineykin, and Ekman layers.

This Ekman layer includes somewhat higher frequencies than the two-term balance Ekman layer in Table 1.

3.3.1. *Thermal Stokes layer.* The flow in the thermal Stokes layer is driven by temperature diffusion. We notice that since $(d^2/d\eta^2 + i\hat{\omega})\, p_s = 0$, it follows that $(d^2/d\eta^2 + i\hat{\omega})\theta_s = 0$ and consequently, from eq. (2) that $w_s = u_s = 0$, where the subscript s identifies the thermal Stokes contribution. Therefore, the Stokes flow is geostrophic and the cross-isobar flow and vertical motion are produced only by the oscillating Lineykin-layer and the Ekman-layer parts of the total solution. The governing equations and general solutions of the thermal Stokes layer are:

$$\left.\begin{aligned} &-v_s = p_s \\ &\frac{\partial p_s}{\partial \eta} = \theta_s \\ &\left(\frac{\partial^2}{\partial \eta^2} + i\hat{\omega}\right) p_s = 0 \quad \text{or} \quad \left[\left(\frac{\partial^2}{\partial \eta^2} + i\hat{\omega}\right)\theta_s = 0\right] \end{aligned}\right\} \tag{13}$$

$$\left.\begin{aligned} P_s &= C_s \exp\left[-\sqrt{\frac{\hat{\omega}}{2}}\,(1 - i)\,\eta\right] \\ \theta_s &= -\sqrt{\frac{\hat{\omega}}{2}}\,(1 - i)\, C_s \exp\left[-\sqrt{\frac{\hat{\omega}}{2}}\,(1 - i)\,\eta\right] \\ v_s &= -C_s \exp\left[-\sqrt{\frac{\hat{\omega}}{2}}\,(1 - i)\,\eta\right] \end{aligned}\right\} \tag{14}$$

where C_s is a constant which will be determined later by application of the boundary conditions to the total solution.

3.3.2. *Oscillating Lineykin layer.* For $\hat{\omega} < 1$, the oscillating Lineykin layer represents regions II and IV in Fig. 1; however, further subdivisions are possible according to the basic governing dynamics; if the diffusive processes play a dominant role compared to temporal changes, which is equivalent to the restriction of $m \gg \hat{\omega}(1 - \hat{\omega}^2)$ (region II-a in Fig. 1), the conventional Lineykin layer is recovered. The governing equations and general solution for this layer with approximation of $O(\hat{\omega}^2)$ are:

$$\left.\begin{aligned} &-v_L = p_L \\ &u_L = \frac{\partial^2 v_L}{\partial \eta^2} \\ &\frac{\partial p_L}{\partial \eta} = \theta_L \\ &m w_L = \frac{\partial^2 \theta_L}{\partial \eta^2} \\ &u_L + \frac{\partial w_L}{\partial \eta} = 0 \end{aligned}\right\} \tag{15}$$

$$\left.\begin{aligned}
p_L &= C_L \exp\,[-\sqrt{m}\eta] \\
\theta_L &= -\sqrt{m} C_L \exp\,[-\sqrt{m}\eta] \\
w_L &= -\sqrt{m} C_L \exp\,[-\sqrt{m}\eta] \\
v_L &= -C_L \exp\,[-\sqrt{m}\eta] \\
u_L &= -m C_L \exp\,[-\sqrt{m}\eta]
\end{aligned}\right\} \qquad (16)$$

where the subscript L indicates the Lineykin layer contribution.

If $m \ll \hat{\omega}(1 - \hat{\omega}^2)$, in which case temporal changes are much larger than the diffusion terms, the oscillating Lineykin layer occurs. The governing equations and general solution for this layer are:

$$\left.\begin{aligned}
&-i\hat{\omega} u_L - v_L = p_L \\
&-i\hat{\omega} v_L + u_L = 0 \\
&\frac{\partial p_L}{\partial \eta} = \theta_L \\
&-i\hat{\omega}\theta_L + m w_L = 0 \\
&u_L + \frac{\partial w_L}{\partial \eta} = 0
\end{aligned}\right\} \qquad (17)$$

$$\left.\begin{aligned}
p_L &= C_L \exp\left[-\left(\frac{m}{1-\hat{\omega}^2}\right)^{1/2} \eta\right] \\
\theta_L &= -\left(\frac{m}{1-\hat{\omega}^2}\right)^{1/2} C_L \exp\left[-\left(\frac{m}{1-\hat{\omega}^2}\right)^{1/2} \eta\right] \\
v_L &= -\frac{C_L}{1-\hat{\omega}^2} \exp\left[-\left(\frac{m}{1-\hat{\omega}^2}\right)^{1/2} \eta\right] \\
w_L &= -i\left(\frac{\hat{\omega}^2}{m(1-\hat{\omega}^2)}\right)^{1/2} C_L \exp\left[-\left(\frac{m}{1-\hat{\omega}^2}\right)^{1/2} \eta\right] \\
u_L &= -\frac{i\hat{\omega}}{1-\hat{\omega}^2} C_L \exp\left[-\left(\frac{m}{1-\hat{\omega}^2}\right)^{1/2} \eta\right]
\end{aligned}\right. \qquad (18)$$

In the oscillating Lineykin layer, adiabatic temperature changes are "balanced" by temporal changes instead of heat diffusion.

3.3.3. *Ekman layer*. Since the governing equations for the Ekman layer are the same as given in eq. (2), the general solutions for this layer are:

$$\left.\begin{aligned}
p_\varepsilon &= \sum_{j=1}^{2} C_j e^{-\mu_j \eta} \\
\theta_\varepsilon &= -\sum_{j=1}^{2} C_j \mu_j e^{-\mu_j \eta} \\
w_\varepsilon &= -\frac{1}{m}\left[\sum_{j=1}^{2} (\mu_j^2 + i\hat{\omega})\mu_j c_j e^{-\mu_j \eta}\right] \\
u_\varepsilon &= -\frac{1}{m}\left[\sum_{j=1}^{2} (\mu_j^2 + i\hat{\omega})\mu_j^2 c_j e^{-\mu_j \eta}\right] \\
v_\varepsilon &= \frac{1}{m}\left[\sum_{j=1}^{2} \{(\mu_j^2 + i\hat{\omega})^2 \mu_j^2 - m\} c_j e^{-\mu_j \eta}\right]
\end{aligned}\right\} \qquad (19)$$

where:

$$\mu_1 \cong \left[\frac{1}{2}\left(1 - \hat{\omega} - \frac{m}{2(1-\hat{\omega}^2)}\right)\right]^{1/2} + i\left[\frac{1}{2}\left(1 - \hat{\omega} + \frac{m}{2(1-\hat{\omega}^2)}\right)\right]^{1/2}$$

$$\mu_2 \cong \left[\frac{1}{2}\left(1 + \hat{\omega} - \frac{m}{2(1-\hat{\omega}^2)}\right)\right]^{1/2} - i\left[\frac{1}{2}\left(1 + \hat{\omega} + \frac{m}{2(1-\hat{\omega}^2)}\right)\right]^{1/2}$$

The factors $\hat{\omega}$ and $m/2(1 - \hat{\omega}^2)$ represent, respectively, the direct influence of accelerations and pressure adjustments on the Ekman layer. If accelerations and stratification are unimportant, then the production of vertical motion by the Ekman layer obeys a simple Ekman pumping law (Charney and Eliassen, 1949). In the next section, we construct the total solution by combining the Ekman, Stokes and Lineykin components through application of boundary conditions.

4. Asymptotic solutions

Direct application of boundary conditions (4) to the solutions (14), (16 or 18) and (19) can determine the constants C_s, C_L, C_1 and C_2 as in Kuo (1973) and Leetmaa (1971). Although solution is possible without further approximation, at least for some regions of the $m - \hat{\omega}$ parameter space, it is physically more illuminating to employ the approximation methods used in Leetmaa (1971) and Allen (1972). With this approach certain boundary conditions may be satisfied, to lowest order, by only one or two of the component solutions (thermal Stokes, Lineykin and Ekman layers).

4.1. *Small forcing frequency*

If $\hat{\omega}(1-\hat{\omega}^2) \ll m$, then the time change term in the thermodynamic equation can be neglected (case II-a, Fig. 1; Lineykin layer, Table 1). With the somewhat more restrictive condition

$$[\hat{\omega}(1-\hat{\omega}^2)]^{1/2} \ll \sqrt{m}$$

the low level response of temperature to the surface heating occurs almost exclusively in the Lineykin part of the solution as will be seen below.

This possibility includes significantly stratified mid-latitude circulations driven by interaction of horizontal variations of surface conditions with oscillations on a synoptic time scale. This case also includes flow contributions induced by surface variations approaching steady state as might occur with sea surface anomalies. For relative slow oscillations $[\hat{\omega} \ll m]$ the Stokes layer is much thicker than the Lineykin layer so that the thermal forcing is absorbed primarily by the Lineykin layer. That is, heat diffusion from the surface is compensated by adiabatic cooling in the "relatively" thin Lineykin layer so that temperature changes in the overlying Stokes layer are small. Thus θ_L is $O(1)$ requiring that $C_L = -\theta(0)/\sqrt{m}$. However, the resulting Stokes geostrophic wind is not negligible because the Stokes horizontal temperature gradient and thermal wind occur over a deep layer.

Since the Stokes' cross-isobar flow and vertical motions are zero, the no-slip lower boundary condition for cross-isobar flow and the condition of vanishing vertical motion at the lower boundary can be used to determine the two Ekman coefficients. The no-slip condition for the flow in the geostrophic wind direction determines the coefficient for the Stokes flow. Since the Lineykin and Stokes flows are much larger than the Ekman flow in this direction, this boundary condition states that, to lowest order, the Stokes and Lineykin flows are of opposite sign and comparable magnitude.

The above application of boundary conditions and associated order of magnitude of dependent variables can be shown to be the only possible combination by testing all other possible combinations. For example, if θ_s is also $O(1)$, the resulting large thermal wind shear over the deep Stokes layer would produce a Stokes flow too large to allow satisfaction of the lower boundary conditions. Similarly if θ_ε is $O(1)$ the resulting vertical motion would be too large to satisfy the lower boundary condition.

In summary, the order of magnitude for the dependent variables for the three layers, the boundary conditions and coefficients, are approximately:

$$\left.\begin{aligned}
&\theta_s = O\left(\sqrt{\frac{\hat{\omega}}{m}}\right), \quad \theta_L = O(1), \quad \theta_\varepsilon = O(m)\\
&v_s = O\left(\frac{1}{\sqrt{m}}\right), \quad v_L = O\left(\frac{1}{\sqrt{m}}\right), \quad v_\varepsilon = O(1)\\
&u_L = O(\sqrt{m}), \quad u_\varepsilon = O(1)\\
&w_L = O(1), \quad w_\varepsilon = O(1)
\end{aligned}\right\} \tag{20}$$

$$\left.\begin{aligned}
&\theta_L \simeq \theta(0)\\
&v_L + v_s = 0\\
&w_L + w_\varepsilon = 0\\
&u_L + u_\varepsilon = 0
\end{aligned}\right\} \tag{21}$$

$$\left.\begin{aligned}
&C_L = -\frac{\theta(0)}{\sqrt{m}}\\
&C_s = \frac{\theta(0)}{\sqrt{m}}\\
&C_1 = \frac{\theta(0)(\mu_2 - \sqrt{m})}{\mu_1(\mu_2-\mu_1)(\mu_1^2 + i\hat{\omega})}\\
&C_2 = \frac{\theta(0)(\mu_1 - \sqrt{m})}{\mu_2(\mu_1-\mu_2)(\mu_2^2 + i\hat{\omega})}
\end{aligned}\right\} \tag{22}$$

While the above boundary conditions could be satisfied exactly, the resulting increased complexity would contribute little to the basic behavior of the solutions and at the same time would inhibit physical interpretation of such solutions.

The approximate solutions for the total flow are the sum of the solutions given in eqs. (14), (16) and (19) with constants in eq. (22). The leading-order solutions are:

$$p = \frac{\theta(0)}{\sqrt{m}}\,[e^{-\sqrt{(\hat{\omega}/2)}(1-i)\eta} - e^{-\sqrt{m}\eta} + O(m\sqrt{m})] \tag{23a}$$

$$v = \frac{\theta(0)}{\sqrt{m}}\,[e^{-\sqrt{m}\eta} - e^{-\sqrt{(\hat{\omega}/2)}(1-i)\eta} + O(\sqrt{m})] \tag{23b}$$

$$\theta = \theta(0)\left[e^{-\sqrt{m}\eta} + O\left(\sqrt{\frac{\hat{\omega}}{2m}}\right)\right] \qquad (23c)$$

$$u = \theta(0)\left[\sqrt{m}\, e^{-\sqrt{m}\eta} - \frac{1}{\mu_2 - \mu_1}\right.$$
$$\left.\times \{\mu_1(\mu_2 - \sqrt{m})\, e^{-\mu_1\eta} \quad \mu_2(\mu_1 - \sqrt{m})\, e^{-\mu_2\eta}\}\right] \qquad (23d)$$

For future use we compute the dimensional vertical motion which is

$$w_* = \frac{Kg}{f^2 L^2}\frac{\theta_*(0)}{\theta_{00}}\left[e^{-\sqrt{m}\eta} - \frac{1}{\mu_2 - \mu_1}\right.$$
$$\left.\times \{(\mu_2 - \sqrt{m})\, e^{-\mu_1\eta} \quad (\mu_1 - \sqrt{m})\, e^{-\mu_2\eta}\}\right] \qquad (23e)$$

Note that eqs. (23a) and (23b) do not reduce to the neutrally stratified limit unless some provision is made to let the applied temperature perturbation at the surface approach zero. Such a result was also obtained by Leetmaa (1971) and Stommel and Veronis (1957). Since temporal changes are unimportant in this case, the neglect of the perturbation stratification in the thermodynamic equation is no longer justifiable with vanishing stratification.

We also note that the induced pressure perturbation and the v-flow component in the thermal Stokes layer remain finite as $\hat{\omega} \to 0$, since they are proportional to the vertical integral of the temperature perturbation which is independent of $\hat{\omega}$. As $\hat{\omega}$ decreases, the Stokes temperature perturbation decreases but occurs over an increasing depth.

The profiles of the flow (23d) and (23e) are presented for several different values of the parameter m in Figs. 2 and 3. As the stratification increases, the vertical motion weakens and becomes more bottom trapped. That is, pressure adjustments and resulting compensating divergence become more important within the Ekman layer.

When the value of m is larger than 5×10^{-2}, the vertical velocity (Fig. 3) is reduced by more than 50% of the homogeneous Ekman value.

The solution for vertical motion in eq. (23e) could be viewed as a modified Ekman pumping law by evaluating eq. (23e) at a height determined by the intended depth of the turbulent boundary layer or as determined by conditions of an encompassing numerical model. Evaluation of the solution (23) much above the suspected depth of turbulence has little geophysical application. That is, with slow oscillations, the thermal boundary layer with constant diffusivity may become unrealistically deep. The depth of the thermal boundary layer is not directly constrained by Coriolis effects as is the depth of the momentum boundary layer.

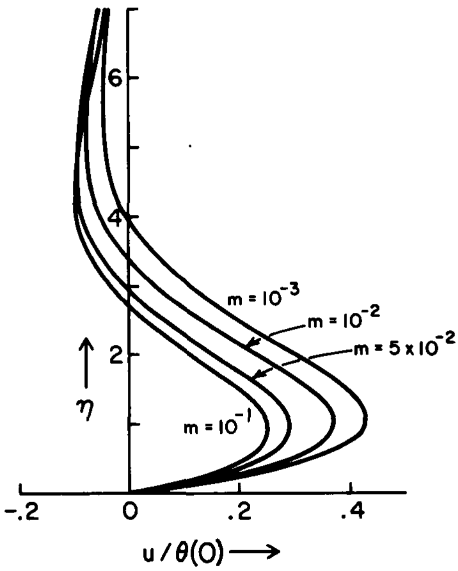

Fig. 2. Scaled amplitude of the cross-isobar flow eq. (23d) as a function of height for several different values of m.

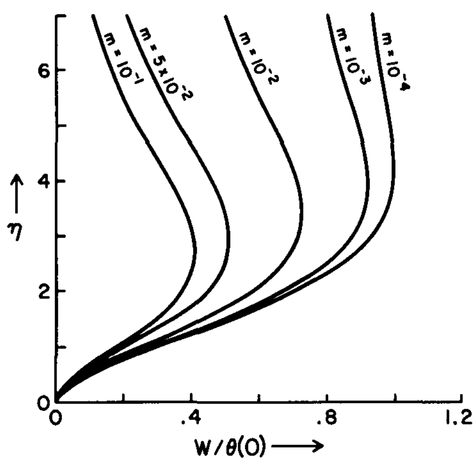

Fig. 3. Scaled amplitude of the vertical velocity eq. (23e) as a function of height for several different values of m.

4.2. *Intermediate forcing frequency*

If the nondimensional forcing frequency satisfies the inequality

$$[\hat{\omega}(1-\hat{\omega}^2)]^{1/2} \gg \sqrt{m} \gg [\hat{\omega}^2(1-\hat{\omega}^2)]^{1/2}$$

the flow is contained in region II-b of Fig. 1. This case can be roughly associated with synoptic-scale oscillations of weaker stratification than Case 1. The condition $\sqrt{m} \ll [\hat{\omega}(1-\hat{\omega}^2)]^{1/2}$ implies that the adiabatic "cooling" (or heating) directly induces temperature oscillations (oscillating Lineykin layer) with temperature diffusion assuming a secondary role. The condition $\sqrt{m} \gg [\hat{\omega}^2(1-\hat{\omega}^2)]^{1/2}$ indicates that the pressure perturbation due to the oscillatory Lineykin layer is larger than that in the thinner Ekman layer. The complimentary case $\sqrt{m} \ll [\hat{\omega}^2(1-\hat{\omega}^2)]^{1/2}$ is discussed in the next sub-section. These subdivisions are presented in Fig. 4.

Using the same order of magnitude analysis as before, we find that:

$$\left.\begin{aligned}
&\theta_s = O(1), \quad \theta_L = O\left(\left[\frac{m(1-\hat{\omega}^2)}{\hat{\omega}}\right]^{1/2}\right),\\
&\theta_\varepsilon = O\left([m\hat{\omega}(1-\hat{\omega}^2)]^{1/2}\right)\\
&v_s = O\left(\frac{1}{\sqrt{\hat{\omega}}}\right), \quad v_L = O\left(\frac{1}{\sqrt{\hat{\omega}}}\right),\\
&v_\varepsilon = O\left(\left[\frac{\hat{\omega}(1-\hat{\omega}^2)}{m}\right]^{1/2}\right)\\
&u_L = O(\sqrt{\hat{\omega}}), \quad u_\varepsilon = O\left(\left[\frac{\hat{\omega}(1-\hat{\omega}^2)}{m}\right]^{1/2}\right)\\
&w_L = O\left(\left[\frac{\hat{\omega}(1-\hat{\omega}^2)}{m}\right]^{1/2}\right),\\
&w_\varepsilon = O\left(\left[\frac{\hat{\omega}(1-\hat{\omega}^2)}{m}\right]^{1/2}\right)
\end{aligned}\right\} \tag{24}$$

$$\left.\begin{aligned}
&\theta_s = \theta(0)\\
&v_s + v_L = 0\\
&w_L + w_\varepsilon = 0\\
&u_L + u_\varepsilon = 0
\end{aligned}\right\} \tag{25}$$

Because the imposed temperature perturbation and resulting temperature diffusion is not balanced by adiabatic cooling but instead produces significant temperature oscillations (thermal Stokes layer), the order of magnitude of the temperature perturbation in the thermal Stokes-layer solution is now larger than that in the Lineykin-layer or Ekman-layer solutions. That is, the Stokes layer is now thinner than the Lineykin-layer and absorbs most of the direct thermal forcing through temperature diffusion. Note that even though u_L and u_ε are of different order, the lower boundary condition is still satisfied since the sine part of the Ekman solution automatically vanishes at the lower boundary. Also note that the non-dimensional vertical velocity is

$$O\left(\left[\frac{\hat{\omega}(1-\hat{\omega}^2)}{m}\right]^{1/2}\right)$$

and thus larger than in case 1. Therefore, accelerations significantly enhance the vertical motion when the adiabatic cooling term does not balance the temperature diffusion and temporal changes are important (Kuo, 1973).

After obtaining coefficients as in case 1, the general solution for case 2, to lowest order becomes:

$$p = \frac{\theta(0)(1+i)}{\sqrt{2\hat{\omega}}}\left[(1-\hat{\omega}^2)\, e^{-\sqrt{m/(1-\hat{\omega}^2)}\eta} - e^{-\sqrt{(\hat{\omega}/2)}(1-i)\eta} + O(\hat{\omega}\sqrt{m})\right] \tag{26a}$$

$$v = \frac{\theta(0)(1+i)}{\sqrt{2\hat{\omega}}}\left[e^{-\sqrt{(\hat{\omega}/2)}(1-i)\eta}\right.$$

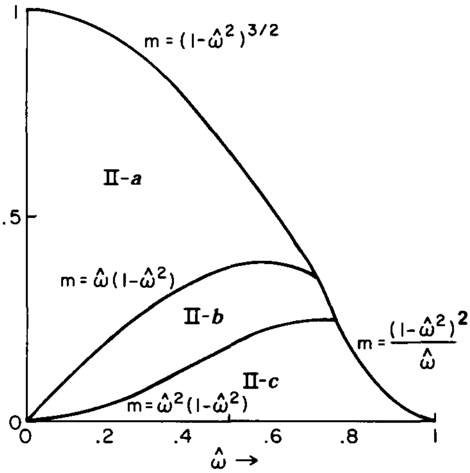

Fig. 4. Subdivisions of the oscillating Lineykin layer in parameter space $(m, \hat{\omega})$. The inequalities defining the three cases in the text are strictly satisfied only in small subspaces of the above three regions.

$$- e^{-\sqrt{m/(1-\hat{\omega}^2)}\eta} + O\left(\left[\frac{\hat{\omega}^2(1-\hat{\omega}^2)}{m}\right]^{1/2}\right)\Bigg] \quad (26b)$$

$$\theta = \theta(0)\left[e^{-\sqrt{(\hat{\omega}/2)}(1-i)\eta} + O\left(\left[\frac{m(1-\hat{\omega}^2)}{\hat{\omega}}\right]^{1/2}\right)\right] \quad (26c)$$

$$u = \sqrt{\frac{\omega}{2}}(1-i)\,\theta(0)\Bigg[e^{-\sqrt{m/(1-\hat{\omega}^2)}\eta} - \sqrt{\frac{1-\hat{\omega}^2}{m}}$$
$$\cdot \frac{1}{\mu_2-\mu_1}\left\{\left(\mu_1\mu_2 - \sqrt{\frac{m}{1-\hat{\omega}^2}}\,\mu_1\right)\right.$$
$$\left.\cdot e^{-\mu_1\eta} - \left(\mu_1\mu_2 - \sqrt{\frac{m}{1-\hat{\omega}^2}}\,\mu_2\right)\cdot e^{-\mu_2\eta}\right\}\Bigg] \quad (26d)$$

The dimensional vertical motion is

$$w_* = \frac{g\theta_*(0)}{f^2 LN\theta_{00}}\sqrt{\frac{K\omega(f^2-\omega^2)}{2}}(1-i)$$
$$\times\Bigg[e^{-(m/(1-\hat{\omega}^2))^{1/2}\eta} - \frac{1}{\mu_2-\mu_1}$$
$$\times\left\{\left(\mu_2 - \sqrt{\frac{m}{1-\hat{\omega}^2}}\right)e^{-\mu_1\eta}\right.$$
$$\left.-\left(\mu_1 - \sqrt{\frac{m}{1-\hat{\omega}^2}}\right)e^{-\mu_2\eta}\right\}\Bigg] \quad (26e)$$

The influence of accelerations on the vertical motion is shown in Fig. 5. As $\hat{\omega}$ increases, the vertical velocity is enhanced by accelerations, but the thickness of the boundary layer does not significantly change.

4.3. *High forcing frequency*

If the nondimensional forcing frequency satisfies the inequality

$$\sqrt{m} \ll [\hat{\omega}^2(1-\hat{\omega}^2)]^{1/2}$$

but is still less than unity, the flow is contained in region II-c of Fig. 4 which includes mid-latitude diurnally-varying motions of synoptic length scale and some meso-scale flows of intermediate or weak stratification. Strongly stratified meso-scale flows might be better described by the dynamics of the

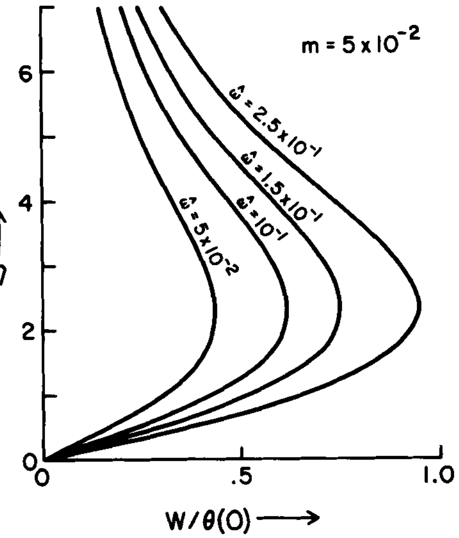

Fig. 5. Profiles of scaled vertical motion for different values of $\hat{\omega}$ and $m = 5 \times 10^{-2}$.

$E^{1/3}$ layer (Table 1). Case 3 also includes oscillations on a synoptic time scale of weak stratification.

The order of magnitude of the variables for each layer and the approximate boundary conditions are:

$$\theta_s = O(1), \quad \theta_\epsilon = O\left(\frac{m}{\sqrt{\hat{\omega}}}\right), \quad \theta_L = O\left(\frac{m}{\hat{\omega}\sqrt{\hat{\omega}}}\right)$$
$$v_s = O\left(\frac{1}{\sqrt{\hat{\omega}}}\right), \quad v = O\left(\frac{1}{\sqrt{\hat{\omega}}}\right),$$
$$v_L = O\left(\left[\frac{m}{\hat{\omega}^3(1-\hat{\omega}^2)}\right]^{1/2}\right) \quad (27)$$
$$u_\epsilon = O\left(\frac{1}{\sqrt{\hat{\omega}}}\right), \quad u_L = O\left(\left[\frac{m}{\hat{\omega}(1-\hat{\omega}^2)}\right]^{1/2}\right),$$
$$w_\epsilon = O\left(\frac{1}{\sqrt{\hat{\omega}}}\right), \quad w_L = O\left(\frac{1}{\sqrt{\hat{\omega}}}\right)$$

$$\left.\begin{aligned} \theta_s &= \theta(0) \\ v_s + v_\epsilon &= 0 \\ u_\epsilon + u_L &= 0 \\ w_\epsilon + w_L &= 0 \end{aligned}\right\} \quad (28)$$

After obtaining coefficients the total solutions become:

$$p = \frac{\theta(0)(1+i)}{\sqrt{2\hat{\omega}}}\left[-e^{-\sqrt{(\hat{\omega}/2)}(1-i)\eta} + \sum_{j=1}^{2} C_j e^{-\mu_j\eta} + O\left(\left[\frac{m(1-\hat{\omega}^2)}{\hat{\omega}^2}\right]^{1/2}\right)\right] \tag{29a}$$

$$\theta = \theta(0)\left[e^{-\sqrt{(\hat{\omega}/2)}(1-i)\eta} + O\left(\frac{m}{\hat{\omega}\sqrt{\hat{\omega}}}\right)\right] \tag{29b}$$

$$v = \frac{\theta(0)(1+i)}{\sqrt{2\hat{\omega}}}\left[e^{-(\hat{\omega}/2)^{1/2}(1-i)\eta} + \frac{C_1}{m}\{\mu_1^2(\mu_1^2+i\hat{\omega})^2 - m\} \times e^{-\mu_1\eta} + \frac{C_2}{m}\cdot\{\mu_2^2(\mu_2^2+i\hat{\omega})^2 - m\}e^{-\mu_2\eta} + O\left(\left[\frac{m}{\hat{\omega}^2(1-\hat{\omega}^2)}\right]^{1/2}\right)\right] \tag{29c}$$

$$u = \frac{\theta(0)(1+i)}{\sqrt{2\hat{\omega}}}\frac{\mu_1\mu_2}{f(\mu_1,\mu_2)} \times\left[\sqrt{\frac{m}{1-\hat{\omega}^2}}\,e^{-\sqrt{m/(1-\hat{\omega}^2)}\eta} - \frac{1}{\mu_2-\mu_1} \times\left\{\mu_1\left(\mu_2-\sqrt{\frac{m}{1-\hat{\omega}^2}}\right)e^{-\mu_1\eta} - \mu_2\left(\mu_1-\sqrt{\frac{m}{1-\hat{\omega}^2}}\right)e^{-\mu_2\eta}\right\}\right] \tag{29d}$$

$$w_* = \frac{gK\theta_*(0)}{f^2L^2\theta_0}\left(\frac{f}{2\omega}\right)^{1/2}(1+i)\frac{\mu_1\mu_2}{f(\mu_1,\mu_2)} \times\left[e^{-\sqrt{m/(1-\hat{\omega}^2)}\eta} - \frac{1}{\mu_2-\mu_1} \times\left\{\left(\mu_2-\sqrt{\frac{m}{1-\hat{\omega}^2}}\right)e^{-\mu_1\eta} - \left(\mu_1-\sqrt{\frac{m}{1-\hat{\omega}^2}}\right)e^{-\mu_2\eta}\right\}\right] \tag{29e}$$

where:

$$C_1 = \frac{m\mu_2(\mu_2^2+i\hat{\omega})\left(\mu_2-\sqrt{\dfrac{m}{1-\hat{\omega}^2}}\right)}{f(\mu_1,\mu_2)(\mu_2-\mu_1)}$$

$$C_2 = \frac{m\mu_1(\mu_1^2+i\hat{\omega})\left(\mu_1-\sqrt{\dfrac{m}{1-\hat{\omega}^2}}\right)}{f(\mu_1,\mu_2)(\mu_1-\mu_2)}$$

and

$$f(\mu_1,\mu_2) = (\mu_2+\mu_1)\left\{\mu_1^2\mu_2^2 - m\left(\hat{\omega}i + \frac{m}{1-\hat{\omega}^2}\right)\right\} - \sqrt{\frac{m}{1-\hat{\omega}^2}}\left(\mu_1\mu_2 - \hat{\omega}i - \frac{m}{1-\hat{\omega}^2}\right)(\mu_1\mu_2+m)$$

Here the boundary layer growth is sufficiently inhibited by oscillation frequency that the assumption of constant eddy voscosity is less serious than in cases 1 and 2. The imposed surface temperature perturbation drives the thermal Stokes layer through the thermal diffusion process as in case 2.

However, the vertical velocity is inversely proportional to the square root of the imposed frequency in contrast to the case 2, where it was roughly proportional to the square root of the imposed frequency. Consequently, we expect the maximum vertical velocities to occur in an intermediate parameter region where $m \sim \hat{\omega}^2(1-\hat{\omega}^2)$. That is, in case 2, the isallobaric enhancement of the vertical motion increases with increasing frequency but further increase of $\hat{\omega}$ in case 3 results in the drastic change of the governing dynamics.

Now the induced geostrophic wind in the thermal Stokes layer becomes weaker with increasing frequency since the depth of the layer of thermal diffusion and thermal wind decrease quickly with increasing frequency. With higher frequencies, the thermal influence has less time to propagate before the forcing reverses sign. The effect of reduced geostrophic winds overrides enhancement of cross-isobar flow by accelerations so that the frictionally-driven vertical motion also decreases with increasing frequency. On the other hand, in the corresponding dynamically-driven flow where the horizontal pressure gradient is specified at the top of the fluid (Park, 1978), the vertical motion does not decrease with $\hat{\omega}$ in this parameter region. In the dynamic case, the depths of the various layers are not related to frequency through temperature diffusion. The decrease of cross-isobar and vertical motion production with increasing frequency, for the present case, is illustrated in Figs. 6, 8 and 10.

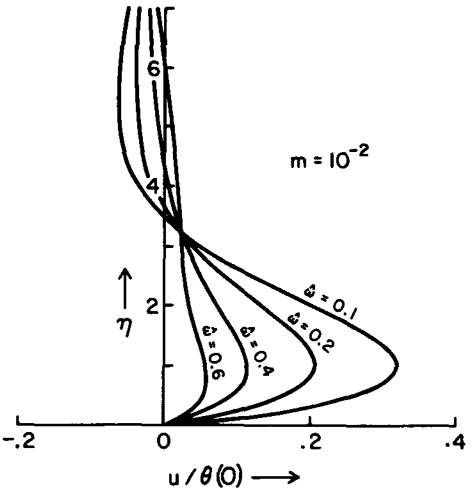

Fig. 6. Scaled amplitude of cross-isobar flow (29d) as a function of scaled height for different values of $\hat{\omega}$ for $m = 10^{-2}$.

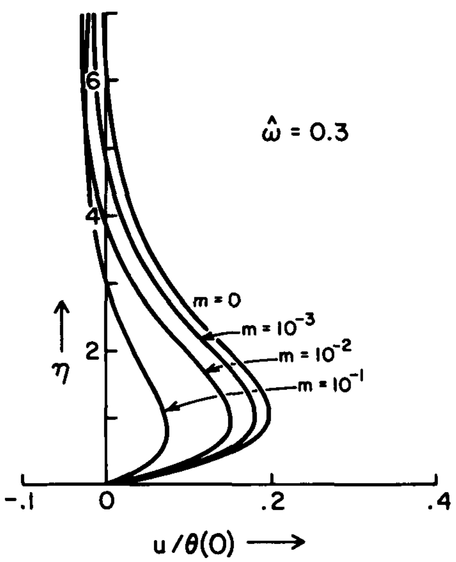

Fig. 7. Scaled amplitude of the cross-isobar flow (29d) as a function of height for several different values of m and $\hat{\omega} = 0.3$.

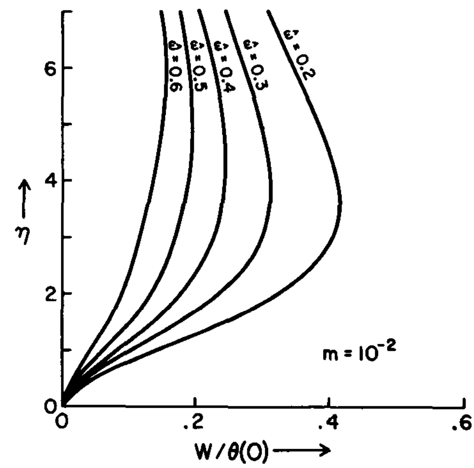

Fig. 8. Scaled amplitude of the vertical velocity as a function of scaled height for several different values of $\hat{\omega}$ and $m = 10^{-2}$.

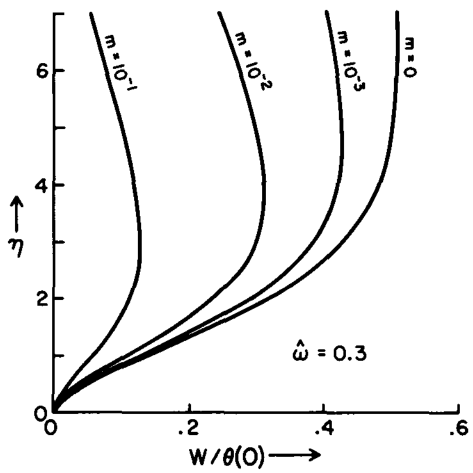

Fig. 9. Scaled amplitude of the vertical velocity as a function of scaled height for several different values of m and $\hat{\omega} = 0.3$.

Figs. 7, 9 and 10 indicate the retarding influence of stratification on vertical motions through pressure adjustments (oscillating Lineykin layer). That is, stratification weakens the boundary layer convergence and concentrates the overlying divergence and return cross-isobar flow to lower levels. The limit of vanishing m should be interpreted as the limit of infinite horizontal length scale. The limit of vanishing basic state stratification is physically not well posed since the influence of the neglected *perturbation* stratification would become important and the assumption of constant eddy viscosity would become particularly serious.

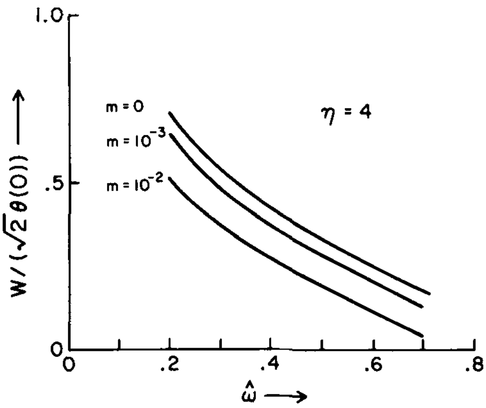

Fig. 10. Scaled amplitude of the vertical velocity versus $\hat{\omega}$ evaluated at the top of the classical Ekman layer, $\eta = 4$, for different values of stratification.

5. Geophysical application

The above study illustrates the influence of accelerations and stratification (through pressure adjustments) on boundary layer production of vertical motion and the depth of the boundary layer. The strength and depth of the cross-iosobar flow and vertical motions of the boundary layer are significantly suppressed by stratification in the lower levels when the non-dimensional stratification parameter $m = N^2K/f^3L^2$ is large compared to the relative oscillation frequency ω/f where f is the Coriolis parameter, L the horizontal length scale, N the Brunt-Väisälä frequency, and K the eddy viscosity. This suppression involves pressure adjustments due to adiabatic temperature changes in the boundary layer. The influence of stratification is most effective (large m) when the horizontal length scale is small. The sensitivity of m to the actual stratification is reduced by an inverse dependence of the eddy viscosity on stratification (Section 3b). First-order corrections due to the suppression of boundary layer vertical motion by pressure adjustments are included in eq. (23e) for the case of slow oscillation frequency and very small stratification influence ($\omega/f \ll m \ll 1$). Such cases are likely to occur with weakly or moderately stratified synoptic scale flow. When m is large compared to one, the stratification influence is dominant and the flow is approximately described by the dynamics of the $E^{1/3}$ layer (Table 1).

For a fixed value of m, the influence of stratification is reduced by increasing frequency of oscillation. Excluding very small horizontal length scales, diurnally varying flows are frequently described by the conditions $\sqrt{m} \ll (\omega/f)[1 - (\omega/f)^2]^{1/2}$. Here, boundary layer convergence and vertical motions may be significantly enhanced by isallobaric effects (eq. (26e)) in contrast to the case where $m \gg (\omega/f)$. However, further increases in oscillation frequency results in a net decrease of vertical motions due to decreasing depth of the thermally driven flow. The influence of boundary layer accelerations and pressure adjustments on the production of vertical motion for this case are included in eq. (29e).

In actual geophysical flows, many additional influences, not considered here, will be important including the dependence of the eddy viscosity and stratification on height and on the flow itself, and influences due to advections, terrain irregularities and evolution of larger scale flow. However, the above study isolates certain "frictional-dynamical" interactions which likely make important contributions to more complicated geophysical flows.

For example, land–sea breeze circulations will exhibit certain properties in common with the oscillating Ekman layer and thermal Stokes layers examined in this study while the overlying return flow of land–sea breeze circulations will share some properties with the oscillating Lineykin layer. Then one might expect the depth of the return flow to be roughly proportional to the horizontal length scale and roughly inversely proportional to the square root of the stratification of potential temperature. As a further example, low level nocturnal jets driven by differential surface cooling will also be characterized by some of the physics contained in the idealized boundary layers studied in Section 4.

The above approach can also be used to study boundary layers dynamically forced by oscillating pressure gradients at the top of the fluid (Park, 1978). However, in this case, physical interpretation of the required boundary conditions is not so straightforward.

6. Acknowledgements

The authors gratefully acknowledge Professor John Allen for suggesting the mathematical approach in Section 4 and for making many important suggestions in the course of this work. We also appreciate the comments of the reviewer. This research was supported by the Meteorology Program of the National Science Foundation under Grant DES 73-06540 A01.

7. Appendix

B Stratification parameter
C Coefficient of eddy viscosity relationship
C_D Drag coefficient
C_L Coefficient of Lineykin flow
C_S Coefficient of Stokes flow
C_1 Coefficient of Ekman flow
C_2 Coefficient of Ekman flow
E Ekman number
f Coriolis parameter
g Acceleration of gravity
H Depth of fluid
K Eddy diffusivity
L Horizontal length scale
m Stratification parameter
N Brunt-Väisälä frequency
p Nondimensional amplitude of pressure
$\tilde{p}$ Dimensional pressure
$\hat{p}$ Rescaled pressure amplitude
p_L Lineykin pressure
p_* Dimensional amplitude of pressure
t Scaled time
t_* Dimensional time
u Nondimensional amplitude of eastward flow
$\tilde{u}$ Dimensional eastward flow
$\hat{u}$ Rescaled amplitude of eastward flow
u_* Dimensional amplitude of eastward flow
u_ε Ekman eastward flow
u_L Lineykin eastward flow
V Horizontal velocity scale
v Nondimensional amplitude of northward flow
$\tilde{v}$ Dimensional northward flow
$\hat{v}$ Rescaled amplitude of northward flow
v_* Dimensional amplitude of northward flow
v_ε Ekman northward flow
v_s Stokes northward flow
w Nondimensional amplitude of vertical motion
$\tilde{w}$ Dimensional vertical motion
$\hat{w}$ Rescaled vertical motion amplitude
w_* Dimensional amplitude of vertical motion
w_L Lineykin vertical motion
w_ε Ekman vertical motion
x Scaled eastward coordinate
x_* Dimensional eastward coordinate
z_* Dimensional vertical coordinate
$\alpha_{1,2}$ Ekman coefficients
α_s Stokes coefficient
α_L Lineykin coefficient
δ Height scale
η Nondimensional vertical coordinate
θ Nondimensional amplitude of potential temperature
$\tilde{\theta}$ Dimensional potential temperature
$\hat{\theta}$ Rescaled amplitude of potential temperature
θ_* Dimensional amplitude of potential temperature
θ_0 Height dependent part of basic state potential temperature
θ_{00} Constant basic state potential temperature
θ_ε Ekman potential temperature
θ_L Lineykin potential temperature
θ_s Stokes potential temperature
$\Delta\theta_0$ Potential temperature thickness of basic state flow
μ_1 Ekman coefficient
μ_2 Ekman coefficient
ρ_{00} Basic state density
ω Oscillation frequency
$\hat{\omega}$ ω/f

REFERENCES

Allen, J. S. 1972. Upwelling of stratified fluid in a rotating annulus: steady state. Part 1. Linear theory. *J. Fluid Mech. 56*, 429–445.

Blumsack, S. and Barcilon, A. 1971. Thermally-driven linear vortex. *J. Fluid Mech. 48*, 801–814.

Bonner, William D. and Paegle, J. 1970. Diurnal variations in boundary layer winds over south-centered United States in summer. *Month. Wea. Rev. 98*, 735–744.

Buajitti, K. and Blackadar, A. K. 1957. Theoretical studies of diurnal wind structure variations in the planetary boundary layer. *Quart. J. Roy. Met. Soc. 83*, 486–500.

Charney, J. G. and Eliassen, A. 1949. A numerical method of predicting the perturbations of the middle latitude westerlies. *Tellus 1*, 38–54.

Holton, J. R. 1967. The diurnal boundary layer wind oscillation above sloping terrain. *Tellus 19*, 199–215.

Hsueh, Y. and Kenney III, R. N. 1972. Steady coastal upwelling in a continuously stratified ocean. *J. Phy. Ocean. 2*, 27–33.

Kuo, H. L. 1973. Planetary boundary layer flow of a stable atmosphere over the globe. *J. Atmos. Sci. 30*, 53–65.

Leetmaa, A. 1971. Some effects of stratification on rotating fluids, *J. Atmos. Sci. 28*, 65–71.

Park, S. U. 1978. Influence of stratification and accelerations on boundary layer production of vertical motion. Ph.D. thesis, Dept. of Atmospheric Sciences, Oregon State University, Corvallis, Or. 97331.
Stommel, H. and Veronis, G. 1957. Steady convective motion in a horizontal layer of fluid heated uniformly from above and cooled nonuniformly from below. *Tellus 9*, 401–407.
Zilitinkevich, S. S., Laikhtman, D. L. and Monin, A. S. 1967. Dynamics of the atmospheric boundary layer. *Izv. Akad. Nauk. SSSR, Fiz. Atmos. Obcana 3*, 1069–1077.

ОСЦИЛЛИРУЮЩИЕ СТРАТИФИЦИРОВАННЫЕ ПОГРАНИЧНЫЕ СЛОИ

Предлагается классификация стратифицированных пограничных слоев вращающейся жидкости, возбуждаемых периодически. Показано, что динамика таких слоев зависит от произведения числа Экмана и параметра стратификации и от отношения частоты возбуждения к параметру Кориолиса. Описан ряд асимптотических решений для величин параметра стратификации, встречающихся в атмосфере, и для суточных и среднеширотных синоптических значений безразмерной частоты возбуждения. Для случая потока, возбуждаемого суточным ходом дифференциального разогрева поверхности, термическое возбуждение поглощается в основном стоксовой частью потока, которая в свою очередь генерирует экмановский слой и связанные с ним вертикальные движения. Эта экмановская накачка вызывает приспособление давления в расположенном сверху осциллирующем слое Линейкина.